AAS 16-240

# RE-ENTRY PREDICTION OF SPENT ROCKET BODIES IN GTO

**David Gondelach[*], Aleksander Lidtke[‡], Roberto Armellin[†], Camilla Colombo[†], Hugh Lewis[†], Quirin Funke[‡], and Tim Flohrer[‡]**

Spent upper stages are bodies consisting of components likely to survive re-entry, for example propellant tanks. Therefore, the re-entry of upper stages might be associated with high on-ground casualty risk. This paper presents a tool for re-entry prediction of spent rocket bodies in GTO based exclusively on Two Line Element set (TLE) data. TLE analysis and filtering, spacecraft parameters estimation, and combined state and parameters estimation are the main building blocks of the tool. The performance of the tool is assessed by computing the accuracy of the re-entry prediction of 92 GTO objects, which re-entered in the past 50 years.

## INTRODUCTION

The geostationary transfer orbit (GTO) is a highly-eccentric orbit with perigee normally at low altitudes (150-650 km) and the apogee near the geo-stationary altitude (35,780 km). Thus, a spent upper stage in a GTO generally passes through the Low Earth Orbit (LEO) and Geostationary Earth Orbit (GEO) regions. Because these regions are both densely populated orbital regimes, a GTO object might collide with an operating spacecraft, damaging it and generating new space debris. In addition, the spent upper stages are large bodies consisting of highly survivable components (such as propellant tanks). Thus, their re-entry might violate the constraint on ground casualty risk.[1,2] In light of the above, the improvement of accurate orbit determination and re-entry prediction of GTO spent upper stages is a key issue to manage both on-orbit collision risk and on-ground casualty risk.

Generally, re-entry prediction is done by propagating an object until it reaches the altitude where atmospheric break-up occurs, typically around 78 km.[3] The main difficulties in this approach are determining the object's initial orbit and correctly modelling the atmospheric drag that is acting on it.

First, the only public data source currently available for determining the orbit of a space object are Two Line Element sets (TLEs), provided by the United States Strategic Command (USSTRATCOM). TLEs are generated using SGP4 (and SDP4) force models[4] which are based on the Brouwer theory[5] and only include the largest perturbations: $J_2$ to $J_5$ zonal harmonics, simplified drag and third body and solar radiation pressure. The many assumptions can severely limit the accuracy of SGP4 propagation. Because many of short-periodic perturbations are not taken into account, the maximum possible accuracy is limited.[6]

[*]Astronautics Research Group, University of Southampton, SO17 1BJ, Southampton, United Kingdom, david.gondelach@soton.ac.uk

[†]Astronautics Research Group, University of Southampton, SO17 1BJ, Southampton, United Kingdom

[‡]European Space Operations Center, European Space Agency, Robert-Bosch-Str. 5, 64293 Darmstadt, Germany

Second, the perturbing acceleration due to atmospheric drag depends on the spacecraft's drag coefficient, $C_d$, area-to-mass ratio, $A/m$, velocity with respect to the atmosphere, $v$, and on the atmospheric density, $\rho$, where $C_d A/m$ can be combined into the ballistic coefficient, BC:

$$\ddot{r}_{drag} = \frac{1}{2} C_d \frac{A}{m} \rho v^2 \tag{1}$$

The drag coefficient is generally uncertain and the area-to-mass ratio depends on the object's attitude which is often unknown. The local atmospheric density, on the other hand, depends on the solar and geomagnetic activity that are hard to predict. As a result, the acceleration acting on a space object due to drag is difficult to compute accurately.

The European Space Agency funded a study to improve the re-entry prediction of upper stages in GTOs. This study is split in two main parts:

1. Improving TLE based re-entry predictions for upper stages in GTOs.
2. Optimising observation strategies to improve the orbit determination of upper stages in GTOs.

This paper discusses part one: re-entry time of objects in GTO based on TLEs. Here the main constraint is that only orbital data from TLEs can be used.

For predicting the re-entry date of an object by propagating its state until re-entry, one requires a force model, parameters to model the object and the initial state of the object. The ballistic coefficient and state of an object derived from TLE correspond to the SGP4 force model and are not meant for use with a different propagator, which is needed for accurate predictions. Therefore, the BC and state are estimated using the object's orbital data provided by TLEs to obtain estimates suitable for use with an accurate propagator. For this purpose, incorrect and poor-quality TLEs need to be filtered out. This results in the following four steps for improved TLE-based re-entry prediction:

1. *Analysis of TLE data*: TLEs for objects in GTO are less accurate compared to TLE for other types of orbits.[7,8] In addition, the quality of TLEs associated to an object is not homogeneous: sometimes low quality or even wrong TLEs are distributed. For this reason, analysis of TLEs is needed to identify outliers and TLEs of poor quality.

2. *BC estimation through TLE data*: TLEs do not provide information on object parameters, such as the ballistic coefficient: $BC = C_d A/m$. A parameter $B^*$ is included in TLEs which is an SGP4 drag-like coefficient.[9] A true BC can be recovered from the $B^*$ term: $BC = 12.741621 B^*$.[10] However, because of the simplified force modelling, a $B^*$ can soak up force model errors during TLE generation.[9] Consequently, the $B^*$ term may not provide a representative value for the true BC. Therefore, the need to estimate the object parameters required for drag modelling arises.[11,12,13] Besides, one can also estimate the object parameters that are required for computing the SRP perturbation.[13] These parameters can be condensed into the SRP coefficient, $SRPC = C_R A/m$, where $C_R$ is the reflectivity coefficient.

3. *State estimation through TLE data*: Re-entry prediction is done by propagating the object's motion until it reaches the altitude where it re-enters. For this, an initial state of the object is required. TLEs can be used to obtain a state directly using SGP4/SDP4, however, with limited accuracy, e.g. Kelso[14] found a mean range error of 10 km with a one-sigma of 5 km

at the epoch of the TLE. For this reason, a better estimate for the initial state is required to do accurate re-entry predictions.[13]

4. *Prediction of re-entry date by accurate orbit propagation*: An orbital propagator with high-fidelity models for the main perturbing forces is required to accurately predict the re-entry date.

The methods used in this approach are discussed in the following section. After that results of the BC and state estimation methods and re-entry prediction are presented, where the sources of poor results are identified and recommendations to do accurate predictions are given.

## METHODS

The steps required for improved TLE-based re-entry prediction are TLE filtering, BC estimation and initial state estimation. Besides, a high-accuracy orbital propagator is required to propagate the object to achieve accurate re-entry predictions. These methods and the orbital propagator are discussed in the following.

### TLE filtering

The TLEs have to be filtered because incorrect, outlying TLEs and entire sequences thereof are expected, and using such aberrant TLEs in subsequent analyses would deteriorate the accuracy of the results. Filtering out aberrant, or incorrect, TLEs consists of a number of stages, namely:

1. Filter out TLEs that were published but then subsequently corrected
2. Find large time gaps between TLEs
3. Identify single TLEs with inconsistent mean motion, as well as entire sequences thereof, using a sliding window approach
4. Filter out outlying TLEs in perigee radius
5. Filter out outlying TLEs in inclination
6. Filter out TLEs with negative $B^*$

It is not uncommon for a TLE to be released soon after a previous one when the orbital elements in the TLE have been corrected. If two TLEs were published shortly after each other, the newer, corrected TLE should be chosen for analysis.[15] Kelecy et al.[16] filter TLEs so that only one element set is left in a 24-hour window, whereas Lemmens and Krag[15] use half an orbital period. Based on statistical analysis of TLE time separations, it was chosen to use half an orbital period as threshold to filter out corrected TLEs.

The TLEs for an object were divided in different sequences by detecting large time gaps and events such as explosions, collisions or periods of increased solar activity. This is because TLEs separated by a large time gap or event should not be used together for BC or state estimation. Moreover, a TLE is also considered an outlier if it is both preceded and followed by a large time gap. This is because the consistency of such a TLE cannot be verified (propagation over a large time gap is deemed uncertain). The threshold for detecting large time gaps was determined for each

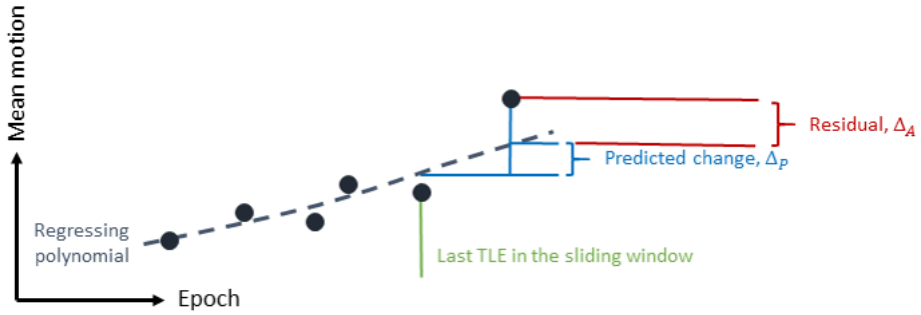


**Figure 1**: Definition of the residual, $\Delta_A$, and the predicted change between the regressing function at the epoch of the last TLE in the sliding window and the following TLE, $\Delta_P$, used to define the relative threshold, $T_R$.

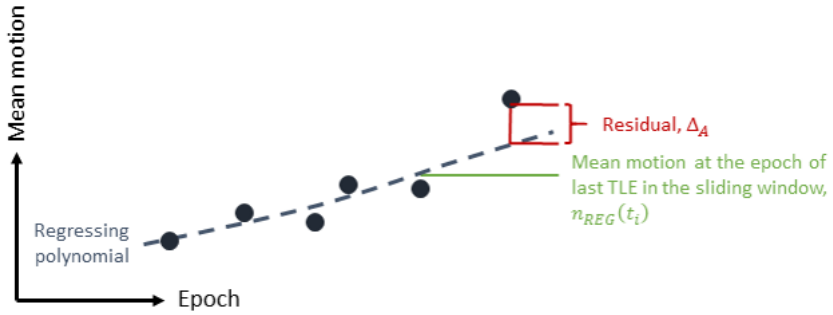


**Figure 2**: Definition of the residual, $\Delta_A$, and the value of the regressing function at the epoch of the last TLE in the window, $n_{REG}$, used to define the absolute threshold, $T_A$.

object separately, because the temporal density of TLEs can vary significantly between different objects.

For the detection of outliers in mean motion, a sliding window approach was implemented. Here the TLE following the sliding window is compared with the regressing function established within the window.[15] The sliding window is restarted if a large time gap is encountered. The regression function is established using Theil-Sen-Seigel *robust* linear regression to reduce the impact of outlying TLEs.[15] A TLE is classified as outlier if two thresholds are exceeded:

1. relative tolerance, $T_R$: the difference between the TLE and the regression, $\Delta_A$, is compared with the predicted change according to the regression function, $\Delta_P$:
   $T_R = \Delta_A / \Delta_P$ (see Figure 1)

2. absolute tolerance, $T_A$: the difference between the TLE and the regression, $\Delta_A$, is compared with the regression mean motion at the end of the window, $n_{REG}$:
   $T_A = \Delta_A / n_{REG}$ (see Figure 2)

The absolute threshold is used to prevent the filter to mark good TLEs as outliers if the change in mean motion, $\Delta n_{REG}$, is very small. The settings that give the best filtering results are a window length of 3 TLEs, and an absolute and relative tolerance of 0.005 and 0.6, respectively.

Besides, corrected TLEs and TLE outliers in mean motion, certain TLEs are also outlying in eccentricity. Instead of filtering TLEs based on eccentricity, it was chosen to use the perigee radius, because outliers in eccentricity are more evident when the perigee radius is examined. Due to the amount of noise in eccentricity of consecutive TLEs, the previously described sliding window approach is less robust in detecting outliers in this orbital element. Therefore, a simple filter was implemented that computes the moving median of the perigee radius and filters out the TLEs that are more then three standard deviations away from this median. Here the standard deviation is computed with respect to the median, not the arithmetic mean. This algorithm was also applied to filter the TLEs in inclination. A threshold of four standard deviations is used in this case, because there are few TLE outliers in inclination, all of which are associated with large discrepancies between their neighbouring TLEs.

Finally, TLEs with negative $B^*$ are filtered out, because they produce SGP4 propagations where the semi-major axis increases, which is not realistic.

**Numerical propagator**

For the re-entry prediction, and ballistic coefficient and state estimation, an orbital propagator is needed. The propagator used in this study is the Accurate Integrator for Debris Analysis (AIDA).[17] This high-precision numerical propagator is tailored for the analysis of space debris dynamics, using up-to-date perturbation models. AIDA includes the following force models:

- geopotential acceleration computed using the EGM2008 model, up to an arbitrary degree and order for the harmonics;
- atmospheric drag, modelled using the NRLMSISE-00 air density model;
- solar radiation pressure with dual-cone shadow model;
- third body perturbations from Sun and Moon.

NASA's SPICE toolbox* is used both for Moon and Sun ephemeris (DE405 kernels) and for reference frame and time transformations (ITRF93 and J2000 reference frames and leap-seconds kernel). Space weather data is obtained from CelesTrak† and Earth orientation parameters from IERS‡.

**Ballistic coefficient estimation method**

The approach used for the estimation of the BC is based on a method for deriving accurate satellite BCs from TLEs proposed by Saunders.[11] The BC is estimated by comparing the change in semi-major axis between two TLEs to the change in semi-major axis due to drag computed by accurate orbit propagation using an assumed BC. The change in semi-major axis between two TLEs, $\Delta a_{TLE}$, is derived using the double-averaged mean motion, $n$, available in a TLE. Since short-periodic changes are removed from TLE data, $\Delta a_{TLE}$ can be assumed to be purely the secular change caused by atmospheric drag. In addition, the orbit is propagated between the two TLE epochs using a guess for the BC and simultaneously the change in semi-major axis due to drag only, $\Delta a_{PROP}$, is computed. This change should be the same as the one derived from the TLEs, as they are both due to

*https://naif.jpl.nasa.gov/naif/index.html
†http://www.celestrak.com/SpaceData/sw19571001.txt
‡ftp://ftp.iers.org/products/eop/rapid/standard/finals.data

atmospheric drag only. Any difference between $\Delta a_{TLE}$ and $\Delta a_{PROP}$ is assumed to be caused by a wrong guess of the BC. Because $\Delta a_{PROP}$ depends on the value of the BC, the BC can be estimated by finding the value for which $\Delta a_{PROP}$ equals $\Delta a_{TLE}$. The estimation is done iteratively using the Secant method. The first guess, $BC_1$, for this method is taken from the $B^*$ in the first TLE.

Four changes were made to the original method by Saunders. First, the change in semi-major axis due to drag is computed directly during propagation by integrating the time derivative of semi-major axis due to drag. Secondly, the second guess, $BC_2$, needed for the Secant method is computed by performing one propagation using the first guess and assuming a linear relation between the BC and $\Delta a_{PROP}$:

$$BC_2 = \frac{\Delta a_{TLE}}{\Delta a_{PROP}(BC_1)} BC_1 \tag{2}$$

During the BC estimation process, it may happen that the object re-enters during propagation. Such a re-entry is probably the result of a too-high estimate for the BC. Therefore, the propagation is then repeated assuming a smaller value for BC; namely $90\%$ of the initial value. This is done multiple times if required. Moreover, re-entry during BC estimation can be prevented completely by propagating backward instead of forward.

Finally, the change in semi-major axis derived from TLEs is the change in *mean* semi-major axis whereas from propagation with AIDA the change in *osculating* semi-major axis is obtained. The change in mean and osculating semi-major axis can differ significantly for objects in GTO. To avoid this discrepancy, the mean semi-major axis is computed from the osculating values and is used for comparison instead of the osculating semi-major axis. Here, the mean is computed by fitting a polynomial through the average value of the semi-major axis per orbital period.

Besides estimating the BC also the SRPC can be estimated, as was done by Dolado-Perez et al.[13] The BC and SRPC are estimated simultaneously by comparing semi-major axis and eccentricity data from TLE with the change in semi-major axis and eccentricity due to drag, SRP and conservative forces.

**State estimation method**

To estimate the initial state of the rocket body, an orbit determination method has been implemented, similar to the methods described by Levit and Marshall,[18] Vallado et al.[19] and Dolado-Perez et al.[13] TLEs are used to generate pseudo-observations and the initial state is estimated by fitting accurate orbit propagation states to the observations using a non-linear least-squares (LSQ) algorithm (lsqnonlin[20]). The process is done as follows.

*Orbit determination process* First, pseudo-observations are derived from TLEs using SGP4[4,9]. The number of observations and length of the observation period can be specified, as well as the coordinates in which the observations are expressed. After that, an initial state guess is generated from one TLE using SGP4. Using this initial state, the assumed object parameters and the generated pseudo-observations, a LSQ algorithm is run to improve the state estimate. The residuals are computed by propagating the object in the observation window and calculating the differences between the propagated orbit and the pseudo-observations at the observations epochs. Based on the residuals and the corresponding Jacobian the initial state is updated such that the propagated orbit fits better with observations.

*Settings* The result of the orbit determination mainly depends on two elements, namely the residuals and the Jacobian. The Jacobian contains the partial derivatives of the residuals with respect

to state components and is required to steer the solution of the LSQ problem. The residuals, on the other hand, determine the objective function value which is minimized by the LSQ algorithm. The values of the residuals therefore directly affect the solution of the LSQ problem. Finally, the guess of the initial state and object parameters is important, because it affects the speed and direction of convergence.

There are various options to implement the OD algorithm. First, the number of observations and length of observation period can be set and various options exists for generating the pseudo-observations. Also, the epoch of the initial state with respect to the observation period can be chosen, e.g. at the start, end or in the middle of the period. In addition, the coordinates and scaling of the initial state and residuals can be selected. Finally, one could choose whether or not to update the Jacobian. The different options that were implemented are briefly discussed next.

- *Pseudo-observation generation* Pseudo-observations can be generated in the following ways:

  1. Single TLE [SingleTLE]: all observations are generated from one TLE equally spread in time;
  2. Multiple TLEs at TLE epochs [TLEepochs]: each observation is generated using a different TLE at the epoch of the TLE;
  3. Multiple TLEs on uniform grid [Uniform]: the observations are generated on an uniform grid, where the TLE closest to the observation epoch is used to generate the observation.

  Using multiple TLEs to generate observations is less susceptible to TLEs of poor quality, because the impact of a single poor TLE on the solution is reduced. Because the accuracy of SGP4 reduces with propagation time,[14] the observations are generated at most two days away from the TLE epoch.

- *Residual coordinates* A proper choice of the residual coordinates may simplify the LSQ problem by simplifying the relation between the initial state and the residuals and making scaling of the residuals easier. The following coordinates have been implemented:

  1. Cartesian coordinates aligned with the inertial reference frame [Cart]: $(x, y, z, V_x, V_y, V_z)$
  2. Cartesian coordinates aligned with satellite coordinate system in radial, transverse, normal direction [RTN]: $(r, t, n, V_r, V_t, V_n)$
  3. Classical orbital elements [COE]: $(a, e, i, \Omega, \omega, \theta)$
  4. Modified equinoctial orbital elements[21] [MEE]: $(p, f, g, h, k, L)$

  Among the Cartesian coordinates the ones in RTN direction are more suitable to differentiate the sources of errors. This is even easier when orbital elements are used as for example the shape $(a, e)$, orientation $(i, \Omega, \omega)$ and the position in orbit $(\theta)$ can be distinguished. However, orbital elements may also be more sensitive, because a small change in an orbital parameter may cause a large change in the dynamics. The classical elements were implemented as mean elements. This was done to avoid the usage of SGP4 for generating observations by extracting the mean values of the orbital elements directly from TLEs (except for the mean anomaly).

- *Residual weighing* In LSQ optimization the weights used for the residuals are key factor, as they are determinant in the definition of optimality. Improper weighing may give too much weight to certain residuals which causes the solution to converge to an inaccurate state estimate.

- *Initial state epoch* The epoch of the initial state can be set at the start, end or in the middle of the observation period.
- *Initial state coordinates* A proper choice of the initial state coordinates may improve the convergence of the LSQ solution. The same coordinates as for the residuals have been implemented, but osculating values were used for COE.
- *Initial state scaling* In numerical optimisation it is in general useful to work with optimisation variables with same order of magnitude,[22] therefore the initial state vector may need to be scaled.
- *Parameter estimation* Next to the initial state also the BC and SRPC can be estimated.
- *Jacobian* Computing the Jacobian can be time consuming and therefore one may choose to compute the Jacobian only once, and use this "fixed" Jacobian throughout the process. This approach works reasonably well as long as the initial condition is close to the optimal solution.

Figure 3 shows the flow diagram of the re-entry prediction approach. First, the TLEs are filtered and subsequently these are used to estimate the BC, generate pseudo-observations and get an initial state guess. Then the state estimate is refined using orbit determination and finally the state and BC estimate are used to predict the re-entry date.

## TEST CASES

Estimating the BC is required to obtain a good initial guess for the OD. In addition, the BC estimate may be used solely to perform re-entry prediction without state estimation. To determine the quality of the BC estimates, estimates were compared with BC values derived from $B^*$ in TLEs and BCs provided in more accurate satellite data, namely Vector Covariance Messages (VCMs)*.

State estimation is performed to improve re-entry predictions. For this reason, the performance of the state estimation method is assessed by investigating the quality of the resulting re-entry predictions. To measure this quality, the error between the predicted and actual re-entry date is used, which is calculated as follows:

$$\%Error = \left| \frac{T_{predicted} - T_{actual}}{T_{actual} - T_{lastusedTLE}} \right| \times 100 \tag{3}$$

where $T_{predicted}$ is the predicted re-entry date, $T_{actual}$ the actual re-entry date and $T_{lastusedTLE}$ the epoch of the last TLE used for the prediction.

To test the re-entry prediction tool, ESA selected 122 rocket bodies that re-entered in the past 50 years. This makes it possible to compare the predicted re-entry date with the real one. The re-entry dates were taken from satellite decay messages from the Space-Track website† that provide the decay date of space objects. It is worth mentioning that all provided decay times are at midnight and this can produce a bias in the calculated re-entry prediction error. All upper stages were initially in GTOs, but have various re-entry dates, lifetime, inclination and area-to-mass ratio. A subset of 26

*Vector covariance messages are catalog orbital data produced by JSpOC using special-perturbations-based orbit determination and are therefore more accurate than TLE.

†`https://www.space-track.org`

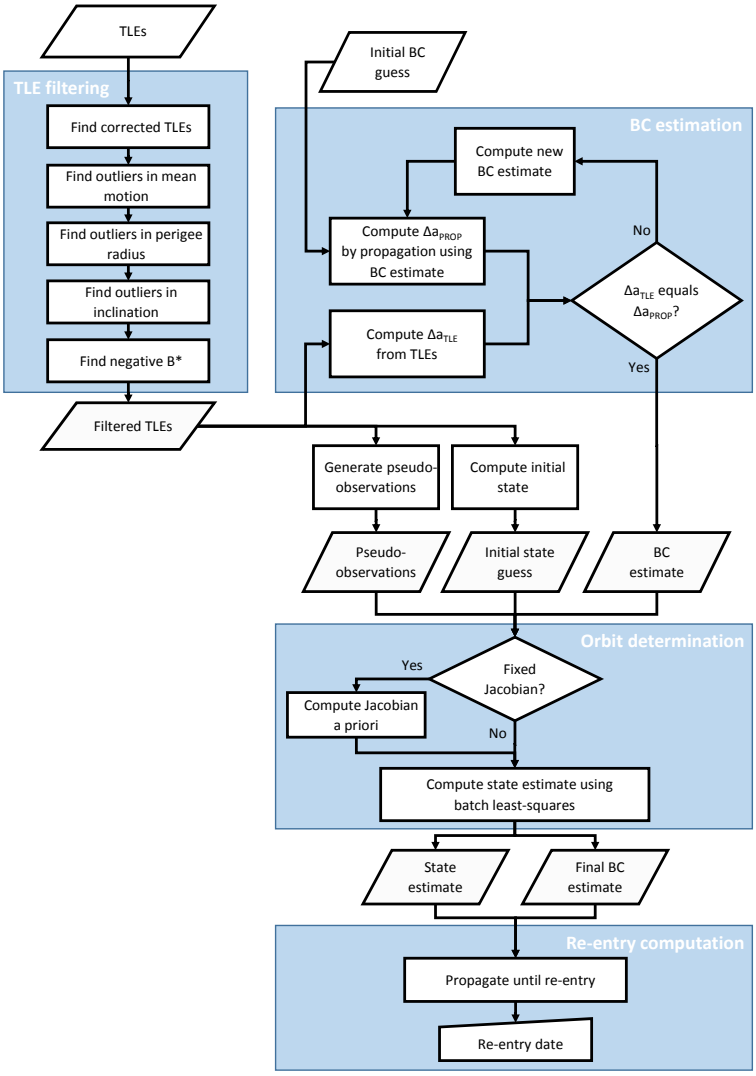


**Figure 3**: Flow diagram of re-entry prediction approach.

objects were selected to perform extensive testing, see Appendix for a detailed list of all test objects. These 26 rocket bodies have been used to test the BC estimation method and to find the best settings for the OD method. In addition, the re-entry of 92 objects has been predicted 30 days before the actual re-entry date. Thirty out of 122 objects were not suitable for this re-entry prediction test, because they had no TLEs, wrong TLEs (available TLEs supposedly do not belong to the object) or no TLEs near 30 days before the re-entry (e.g. last TLE is 180 days before re-entry). For the 92 rocket bodies the perigee altitude 30 days before re-entry varied between 95 and 232 km and the eccentricity between 0.04 and 0.73. To compare the results, the re-entry has been predicted using only an estimate for the BC or after full state estimation.

In real re-entry prediction cases the actual re-entry date of the object is, of course, not known. Analysing the results has therefore not only the goal to examine the quality of the re-entry predictions but also to define guidelines for real re-entry prediction scenarios.

## RESULTS

In this section the results of the BC and state estimation methods and re-entry prediction results using different approaches are discussed.

### BC estimation

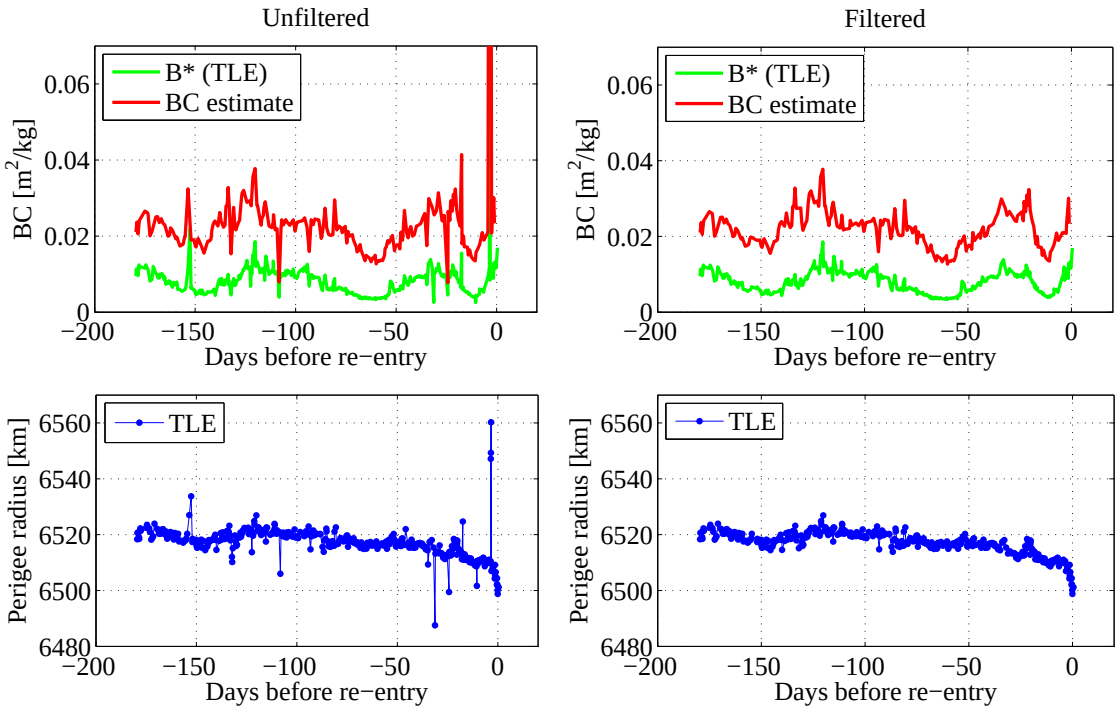


**Figure 4**: BC estimates and BC from $B^*$ from TLE (upper plots) and the perigee radius according to TLE (lower plots) for object 28452 in the 180 days before re-entry. In left plots the TLEs have been filtered on mean motion only and in right plots on mean motion and perigee radius.

Figure 4 shows the BC estimates and BC from $B^*$ for object 28452 together with the perigee radius according to TLE in the 180 days before re-entry. For the left plots TLEs filtered on mean motion were used, whereas for the right plots the TLE were filtered on mean motion and perigee radius. First of all, the trend of the BC estimates is similar to the trend of the BC from $B^*$, but with an offset. This proves that a BC estimate is required in order to perform re-entry prediction with a dynamical model different from SGP4/SDP4. In addition, the BC estimates were compared with BC values contained in VCMs (these are not shown in Figure 4 because of a pending authorization from USSTRATCOM). On average the median of BC estimates for the 26 objects differs 12% from the median of BC from VCM and 75% from BC from $B^*$. Both the BC estimates and BC from VCMs were obtained using high-accuracy (special perturbations) models with accurate atmospheric models. The atmospheric model used for VCM (JAC70 or MSIS90) is however different from the one used here (NRLMSISE-00) which may explain the difference in BC values. This gives confidence that the estimation method provides good results.

Furthermore, there is a clear correlation between outliers in TLE perigee radius and estimated BC; an outlier in perigee radius results in an outlier in the BC estimates. More precisely, an outlier in

the first TLE used for the BC estimation results in an outlier in BC estimate. This can be explained by the fact that the first TLE is used to derive the initial state used for propagation, whereas the second TLE is only used to compute the change in semi-major axis according TLE. Therefore, it can be concluded that the BC estimate depends strongly on the initial state used in the estimation. Because the atmospheric drag depends largely on altitude, an incorrect value of the initial state, that translates in an aberrant perigee height, results in a poor BC estimate. The $B^*$ is strongly correlated to the perigee height and thus both the BC estimate and $B^*$ depend on the initial state. As a result the BC estimate and $B^*$ follow the same trend.

The right plots in Figure 4 show the BC estimates and perigee radius after filtering the TLEs on outliers in perigee radius. Clearly, the BC estimates improve, because outliers in BC estimate disappear when TLE outliers in perigee radius are removed. Nevertheless, there are still small outliers in the BC estimate visible, which may be removed when also smaller outliers in perigee radius are filtered out.

This proves that to obtain a good single BC estimate the TLEs should be filtered on perigee radius, or on both semi-major axis and eccentricity. Another option to avoid the impact of outliers on the estimate would be to do multiple BC estimates and take the median of the estimates as final BC estimate. In the current approach only one BC estimate is computed, because the estimation of multiple BCs was considered time consuming.

Next the BC estimation method, also the method for estimating the BC and SRPC was implemented and tested. In all test cases the orbit has a low perigee altitude and therefore the effect of SRP was at least an order of magnitude smaller than the effect of drag. This resulted in an ill-conditioned system of equations for estimating the BC and SRPC and consequently gave aberrant results for the SRPC. Therefore, it was chosen not to estimate the SRPC, but instead to computed the SRPC by using the same area-to-mass ratio that is used for drag calculations and assuming typical values for the reflectivity and drag coefficients: $C_R = 1.4$ and $C_d = 2.2$.

**Full state estimation**

First, the state estimation method was tested to identify good settings. After that, the accuracy of the method was tested by performing re-entry predictions.

The BC estimation results showed that the BC estimate depends strongly on the initial state. Therefore it was chosen to always re-estimate the BC in the OD process.

First, initial re-entry prediction tests were run to obtain good scaling and weighing factors for the initial state and residuals. After that, predictions were done using all implemented options for pseudo-observation generation, initial state location and residual coordinates with observation windows of 5, 10 and 20 days and with 11 or 21 observations. These tests showed that pseudo-observations generated using only a single TLE is most robust, i.e. least failures occurred during OD, but gives poor predictions and therefore this option was discarded. In addition, observation windows of 10 or 20 days did not gave better results than a 5-days window. Therefore a 5-day window was selected to reduce computational times. Also, the number of observations was set to 21, because that gave better predictions then using 11 observations.

Furthermore, it was found that expressing the initial state in the equinoctial elements gives best results regarding the number of iterations required by the LSQ algorithm and the obtained average position residuals considering all possible residual coordinates. Moreover, the option of inertial Cartesian coordinates for residuals was discarded, because it is similar to the RTN Cartesian co-

ordinates, but the RTN option performed better. Also, locating the initial state at the start of the observation period was dropped as an option, since it is similar to placing the initial state at the end of the period, but results in a larger prediction period.

**Table 1**: Average re-entry prediction error and number of failures for different settings based on re-entry prediction of 26 objects; *average error of best 23 predictions to exclude failures from the average, †pseudo-observations are raw orbital elements from TLE.

| | | Backward | | Midpoint | |
|---|---|---|---|---|---|
| | | Average re-entry prediction error [%]* | # of failures | Average re-entry prediction error [%]* | # of failures |
| TLEepochs | RTN | 13.3 | 3 | 8.7 | 3 |
| | MEE | 12.5 | 3 | 12.4 | 1 |
| | COE† | 11.7 | 2 | 12.7 | 1 |
| Uniform | RTN | 12.8 | 1 | 7.8 | 0 |
| | MEE | 18.3 | 1 | 12.9 | 0 |
| | COE | 21.1 | 1 | 14.7 | 0 |

For determining the best settings for the location of the initial state (midpoint or end of observation period), the coordinates of the residuals (RTN, MEE or COE) and observation epochs (TLEepochs or Uniform) re-entry predictions were done for the 26 selected objects 30 days before re-entry. Table 1 shows the average re-entry prediction error and number of failures obtained using different settings. Here, failure means that the OD did not find a solution. In addition, the average prediction error is computed using the best 23 predictions such that failures are not included in the average. Clearly, the best predictions are obtained when the initial state is located at the midpoint of the observation period. Considering only the pseudo-observation generation, observations at TLE epochs gives better predictions, however, applying observations on an uniform grid is more robust as it results in less failures during the OD. Using position and velocity in radial, transverse and normal for expressing the residuals results in the lowest prediction error. Overall, the best predictions were obtained with the observations equally spaced in time together with residuals in RTN coordinates and the initial state at the midpoint. The best combination of settings is reported in Table 2.

**Table 2**: Best settings for OD algorithm; $^*a_0$ is semi-major axis of initial state guess, $^\dagger V_{c,0}$ is orbital velocity at $a_0$; all units in km, s and rad, only BC in kg/m$^2$.

| **Option** | **Best setting** |
|---|---|
| Initial state | MEE and BC $[p, f, g, h, k, L, BC]$ |
| Initial state scaling | $[a_0, 1, 1, 1, 1, 2\pi, 0.5]^*$ |
| Initial state location | Midpoint of observation period |
| Residual coordinates | RTN $[r, t, n, V_r, V_t, V_n]$ |
| Residual weighing | $[a_0; a_0; a_0; V_{c,0}; V_{c,0}; V_{c,0}]^\dagger$ |
| Pseudo-observations | 21 observations equally-spaced in 5 days period,<br>TLE closest to obs epoch is used to generate observation |

The advantage of using observations on an uniform grid compared to observations at TLE epochs

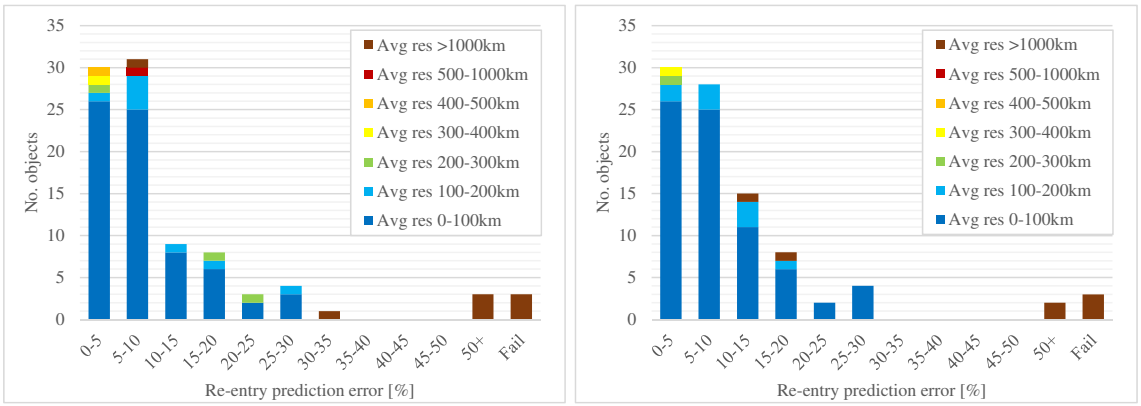


(a) Errors using OD with fixed Jacobian.

(b) Errors using OD with updated Jacobian.

**Figure 5**: Histogram of re-entry prediction errors for 92 objects 30 days before re-entry using OD with (a) fixed and (b) updated Jacobian. The different colours in the histogram correspond to results with different average position residuals.

is that there are more observations and that the observations are distributed equally around the initial state. On the other hand, generating the observations at the TLE epoch has the benefit that the impact on the solution is equal for each TLE, because for each TLE the same number of pseudo-observations are generated. Besides, when generating observations at the TLE epochs, SGP4 propagation is only used at $t_0$ which can be advantageous, e.g. when the $B^*$ value is poor. The fact that locating the initial state in the middle of the observation period works best seems logical. Propagation errors grow in time and consequently residuals located further away from the initial state will generally be larger. By locating the initial state in the middle this effect is balanced.

***Fixed vs updated Jacobian*** Besides the settings shown in Table 2, one can choose to fix the Jacobian during the OD or update it at every iteration step. To investigate the effect of fixing the Jacobian, the re-entry of 92 objects was predicted 30 days before re-entry. Here the number iterations for the LSQ algorithm was limited to 30. Histograms of the re-entry prediction errors obtained using a fixed or updated Jacobian are shown in Figure 5. The improvement of the results with updating the Jacobian can be seen by the increase in predictions with an error between 10-15% and decrease in predictions with an error 20-25% and >30%. Besides these improvements, a decrease in the number of predictions with an error between 5-10% can be noticed. This is because some predictions are a few percent worse compared to the fixed-Jacobian result, simply because a better OD fit does not necessarily translate into a better re-entry prediction. On average, the prediction accuracy improved by 0.5%. This improvement comes at the cost of computational speed. Each LSQ iteration step is 8 times slower compared to using a fixed Jacobian, because 7 additional orbit propagations are required for updating the Jacobian (one for each element in the initial state vector).

***Comparison*** Figure 6 shows the cumulative distribution of the re-entry errors for re-entry predictions using only an estimate for the BC or after full state estimation with fixed or updated Jacobian (with the settings of Table 2). Clearly, the re-entry predictions after OD are much better. 50% of all re-entry predictions using OD with a fixed and updated Jacobian have an error less than 7.6% and 7.1%, respectively. A re-entry prediction error less than 20% is achieved by 85% and 88% of the results using a fixed or updated Jacobian, respectively. On the other hand, when only the BC is

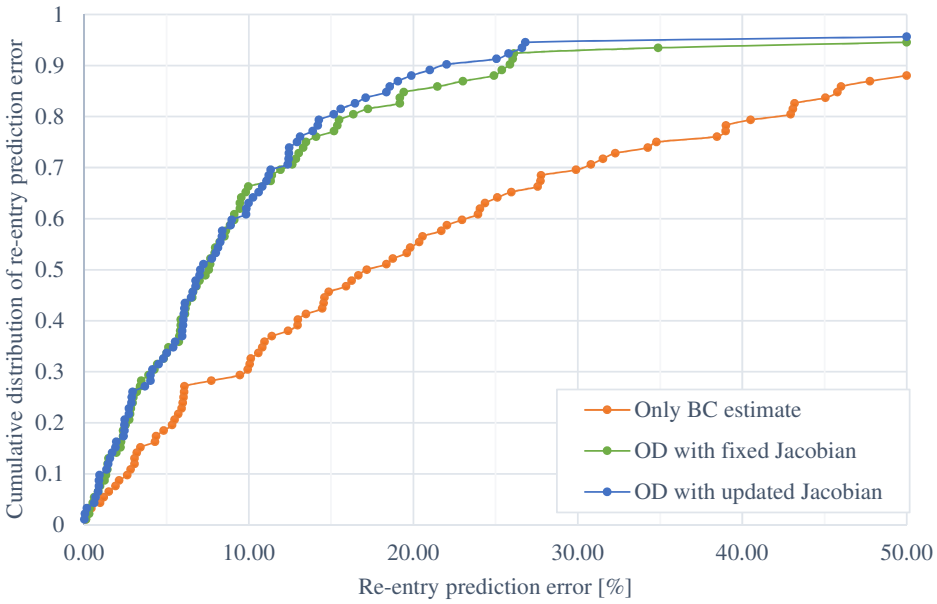


**Figure 6**: Cumulative distribution of re-entry prediction error of 92 objects 30 days before re-entry using only an estimate for BC and using OD with fixed and updated Jacobian.

estimated, then only 54% of the results is within 20% error. Thus, as expected, re-entry prediction using OD outperforms predictions using only an estimate for the BC. Besides, applying an updated Jacobian mainly improves the results with a high prediction error, since the best 60% of the results using fixed and updated Jacobian are similar. With almost 90% of the results within 20% error and more than 60% of the predictions within 10%, the presented re-entry prediction method provides quite reliable re-entry predictions considering the quality of TLEs.

## Discussion

***High residuals*** It was found that when the fit of the orbit is poor then usually the re-entry prediction is poor as well. The OD results for which the average position residual between the estimated orbit and observations is larger than 500 km are shown in red and brown in Figure 5. All predictions with an error larger than 30% have an average position residual that is more than 500 km. In the updated Jacobian case, there are two results at 10-15% and 15-20% with an average residual larger than 500 km. These two results actually correspond to two results which were at 30-35% and 50+% in the fixed Jacobian results (Figure 5a). Thus, it is suggested to run the OD with an updated Jacobian when the fixed option produces residuals with an average position residual larger than 500 km. If the residuals then decrease significantly, the re-entry prediction is probably better as well. The experience is that if the average residual is much larger than 500 km then the predicted re-entry date should not the trusted.

***Failures*** In three cases the OD algorithm was not able to find a solution, because the object re-entered during propagation causing the LSQ algorithm to fail. This happens when the TLEs and/or initial state guess are of poor quality, causing the LSQ algorithm to compute a solution that re-enters within the observation window. In general, failures can be avoided by using the SingleTLE option,

because one TLE provides consistent pseudo-observations.

***Poor predictions*** Poor predictions are in general the result of scarce TLEs or poor quality of the TLEs. The solutions with high residuals and failures in Figure 5 occurred because the number of TLEs in the window was small (less than four) or because the SGP4 propagations of different TLEs were inconsistent (e.g. the gradient of the semi-major axis does not agree). The issue of few TLEs may be resolved by extending the observation period such that it contains more TLEs; a minimum of 4 TLEs is recommended. However, extending the window can result in large time gaps between subsequent TLEs with the risk that the SGP4 propagations of the two subsequent TLEs do not agree. If the pseudo-observations do not agree, then the orbit determination will become more difficult and erroneous. For this reason, large time gaps between TLEs in the observation period should be avoided. A time-gap limit of 5 days can be used, because for all cases with a time gap larger than 5 days poor results were obtained. Ultimately, a single TLE can be used for re-entry prediction if within 5 days no other TLEs are available.

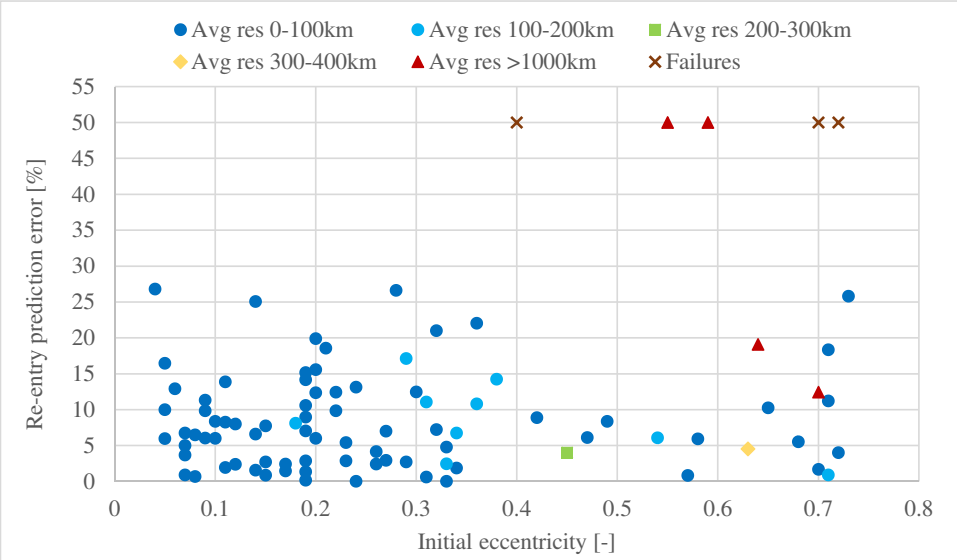


**Figure 7**: Re-entry prediction error of 92 objects against the eccentricity 30 days before re-entry (using OD with updated Jacobian).

***High eccentricity*** Figure 7 shows the re-entry prediction errors plotted against the eccentricity of the orbit 30 days before re-entry. Clearly, the average position residual is low when orbit determination is done for objects in a low eccentricity orbit ($e$<0.25). All results with a high average position residual (>200km) and all failures, on the other hand, occur for orbits with a high eccentricity ($e$>0.4). These results are related to the fact that TLE uncertainties are higher for highly elliptical orbits.[7,8]

***Weighing transverse components*** In total, there were seven re-entry predictions using an updated Jacobian for which the average position residual was larger than 500 km or for which the OD failed, see Figure 5b. For three of these cases it was possible to improve the prediction by given a different weight to the transverse position and velocity residuals, see Table 3. For highly-eccentric orbits the velocity in transverse direction can be very high compared to the radial and normal velocity. This is mainly the case around perigee where the transverse velocity is high and it can result

**Table 3**: Re-entry prediction errors and average position residuals for applying standard and reduced weight to transverse residuals. For these seven objects the OD result had an average position residual >500 km or was a failure using standard weighing.

| | | Re-entry prediction error [%] | | Average position residual [km] | |
|---|---|---|---|---|---|
| NORAD ID | Eccentricity | Standard weighing | Transverse weighing | Standard weighing | Transverse weighing |
| 23797 | 0.70 | 12.4 | 2.3 | 1727 | 2132 |
| 37949 | 0.64 | 19.1 | 24.2 | 1245 | 1507 |
| 25051 | 0.55 | >50 | 15.5 | 8232 | 312 |
| 18923 | 0.59 | >50 | Failure | 13219 | - |
| 21057 | 0.40 | Failure | Failure | - | - |
| 23916 | 0.70 | Failure | Failure | - | - |
| 22932 | 0.72 | Failure | 12.9 | - | 136 |

in large position residuals in transverse direction. Around perigee the radial residuals can however be considered more important, because they are closely related to the perigee altitude which is has more impact on the evolution of the orbit on the long term (compared to the in-track position). Therefore, the weighing of the residuals in transverse direction should be reduced so the LSQ algorithm converges to a solution that gives a better initial state for predicting the orbital evolution and therefore the re-entry. The additional weighing of the transverse position and velocity residuals is achieved by scaling using a factor that is proportional to the eccentricity: $1 + 10e$. This is chosen because the effect is stronger at higher eccentricity. Table 3 shows the results of applying additional transverse weighing. For two of the three improved re-entry predictions the average position residual was reduced to less than 500 km, which indicates that the predictions are good.

***Example re-entry prediction*** An example of a re-entry prediction is shown in Figure 8, where the osculating apogee and perigee altitude predicted 39 days before the actual re-entry are plotted. The three different lines show the predictions according to SGP4 (green), using AIDA with only an estimate for the BC (red) and using AIDA after OD (blue) starting at the epoch of the last-used TLE. The SGP4 and BC estimate prediction start at the same altitudes because the BC estimate prediction uses the state derived from TLE using SGP4, whereas the OD prediction starts at the state estimated using OD. Clearly SGP4 cannot correctly represent the dynamics of the orbital decay. The BC-estimate and OD prediction, on the other hand, show a better decay, but in the case of only BC estimation the decay is too steep. The errors in predicted re-entry date after BC estimation and after OD are 46% and 1.7%, respectively. Nevertheless, the values of the estimated BCs after only BC estimation and after OD differ by just 1%. The initial perigee altitude of the BC-estimate and OD prediction however differs by 8 km. The accuracy of the osculating state derived from the TLE is thus clearly not good enough for an accurate re-entry prediction. The OD prediction, on the other hand, corresponds well with future TLEs and obtains a re-entry date which is just half a day off the real date.

## CONCLUSION

A re-entry prediction method based on TLEs has been developed dedicated to objects in GTO. The approach consists of four steps in which subsequently the TLEs are filtered, the ballistic coef-

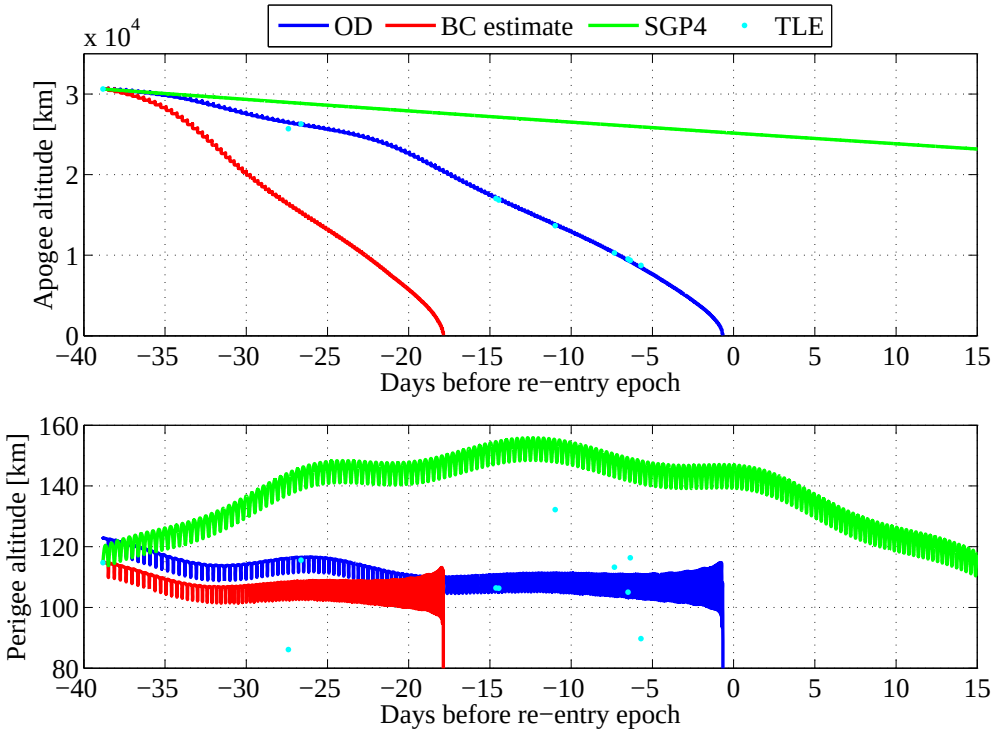


**Figure 8**: Re-entry prediction of object 28239 predicted 39 days before actual re-entry date ($t = 0$). Upper and lower plot show the osculating apogee and perigee altitude, respectively, predicted using OD (blue), BC estimate (red) and SGP4 (green) and according to future TLE (cyan).

ficient and initial state are estimated, and re-entry date is predicted.

TLE filtering was found to be very important, because TLEs of poor quality are the major source of inaccurate BC estimation and orbit determination. Filtering TLE outliers in eccentricity, besides mean motion, is key because the eccentricity determines the perigee altitude that has a large influence on the orbital decay. In addition, TLEs with negative $B^*$ need to be filtered out if SGP4 propagation is used as a negative $B^*$ results in an increase in orbital energy, which is not realistic for decaying objects.

BC estimation results showed that the estimated BC depends strongly on the initial state, because TLE outliers in perigee radius result in outliers in BC estimates.

To estimate the initial state, orbit determination was applied using pseudo-observations generated from TLE. The best and most robust results for re-entry predictions were obtained by using an initial state in MEE, with residuals in RTN coordinates, a 5-day observation window with 21 observations equally-spaced in time, and locating the initial state at the midpoint of the window. Using these settings and an updated Jacobian during OD, 88% of the re-entry predictions had an error less than 20%, compared to 54% of the re-entry predictions using only an estimate for the BC.

The BC was always included during OD, because the BC estimate depends on the initial state. In addition to the BC, also the SRP coefficient may be included in the orbit determination process. This may improve the OD result if a proper weight is applied to the SRPC, especially when the SRP is high.

Analysis of the re-entry prediction results showed that a high average position residual is a good indication that the orbit determination and subsequent re-entry prediction are not accurate. In such cases, the OD can be repeated with an updated Jacobian to obtain better re-entry predictions. Furthermore, the orbit determination and re-entry prediction of objects in high eccentricity orbits was found to be less accurate and less robust then for orbits with low eccentricity. By reducing the weight of position and velocity residuals in the transverse direction the orbit determination for high eccentricity orbits can be improved.

Poor-quality TLEs are the main reason for inaccurate predictions of the re-entry date and for failures of the orbit determination. Besides that, inaccurate predictions are caused by large time gaps between the TLEs used for pseudo-observation generation.

## ACKNOWLEDGEMENT

This work was performed in the framework of the European Space Agency project ITT AO/1-8155/15/D/SR, titled "Technology for Improving Re-Entry Predictions of European Upper Stages through Dedicated Observations". The authors acknowledge the use of the IRIDIS High Performance Computing Facility, and associated support services at the University of Southampton (UoS), in the completion of this work. In addition, the Joint Space Operations Center is acknowledged for providing Vector Covariance Messages for 53 objects used for testing. David Gondelach and Aleksander Lidtke were funded by an EPSRC Doctoral Training Grant awarded by the Faculty of Engineering and the Environment of UoS. Roberto Armellin acknowledges the support received by the Marie Sklodowska-Curie grant 627111 (HOPT - Merging Lie perturbation theory and Taylor Differential algebra to address space debris challenges).

## APPENDIX: TEST OBJECTS

Rocket bodies with the following NORAD catalog numbers were used for re-entry prediction:

625*, 2609, 7252*, 7794*, 8479, 9017, 9859, 10983, 11072*, 11718, 11719, 12562, 12810*, 13025, 13087, 13098, 13136*, 13294, 13447, 13599, 13684, 13940, 14130, 14168, 14287, 14423, 14787, 14989, 15157, 15165*, 15679, 16600, 18352, 18923, 19218, 19332, 19877, 20042, 20123, 20254, 20778, 21057, 21141, 21654, 21766, 21895, 21990*, 22118, 22254*, 22906*, 22928, 22932, 22997*, 23315, 23416*, 23797, 23916, 24314, 24666, 24770, 24799, 24847*, 25051*, 25129*, 25154, 25240, 25313, 25372*, 25496, 25776*, 26560, 26576, 26579, 26641*, 27514, 27719, 27808*, 28185, 28239, 28253, 28418, 28452*, 28623*, 28703, 29497*, 32764*, 37211*, 37239*, 37257, 37764, 37949*, 39499.

The objects indicated with $*$ are the 26 rocket bodies that were used to test the BC and state estimation methods.

## REFERENCES

[1] Inter-Agency Space Debris Coordination Committee, "IADC Space Debris Mitigation Guidelines," September 2007.

[2] NASA, "NASA Technical Standard 8719.14, Process for Limiting Orbital Debris," August 2007.

[3] H. Klinkrad, *Space debris*. Wiley Online Library, 2010.

[4] F. R. Hoots and R. L. Roehrich, "Spacetrack Report No. 3–Models for Propagation of NORAD Elements Sets," *Spacetrack Report*, Vol. 3, No. 3, 1980.

[5] D. Brouwer, "Solution of the problem of artificial satellite theory without drag," *The Astronomical Journal*, Vol. 64, 1959, p. 378.

[6] D. A. Vallado and P. Cefola, "Two-line element sets–practice and use," *63rd International Astronautical Congress, Naples, Italy*, 2012.

[7] T. Flohrer, H. Krag, and H. Klinkrad, "Assessment and categorization of TLE orbit errors for the US SSN catalogue," *Advanced Maui Optical and Space Surveillance Technologies Conference, 17–19 September 2008, Wailea, Maui, USA*, 2008.

[8] T. Flohrer, H. Krag, H. Klinkrad, B. Bastida Virgili, and C. Früh, "Improving ESAs Collision Risk Estimates by an Assessment of the TLE orbit Errors of the US SSN Catalogue," *5th European Conference on Space Debris, Darmstadt, Germany*, 2009.

[9] D. Vallado, P. Crawford, R. Hujsak, and T. S. Kelso, *Revisiting Spacetrack Report #3*, Vol. 6753. 2006, 10.2514/6.2006-6753.

[10] D. Vallado, *Fundamentals of Astrodynamics and Applications*. Space technology library, Microcosm, 2013.

[11] A. Saunders, G. G. Swinerd, and H. G. Lewis, "Deriving Accurate Satellite Ballistic Coefficients from Two-Line Element Data," *Journal of Spacecraft and Rockets*, Vol. 49, No. 1, 2012, pp. 175–184, 10.2514/1.A32023.

[12] M. Mutyalarao and R. K. Sharma, "On prediction of re-entry time of an upper stage from GTO," *Advances in Space Research*, Vol. 47, No. 11, 2011, pp. 1877–1884, 10.1016/j.asr.2011.01.028.

[13] J. Dolado-Perez, L. Aivar Garcia, A. Agueda Mate, and I. Llamas de la Sierra, "OPERA: A tool for lifetime prediction based on orbit determination from TLE data," *24th International Symposium on Space Flight Dynamics Laurel, Maryland, USA, 5–9 May*, Vol. 4, 2014, pp. 123–124.

[14] T. Kelso, "Validation of SGP4 and IS-GPS-200D Against GPS Precision Ephemerides," *17th AAS/AIAA Space Flight Mechanics Conference, Sedona, AZ*, January 2007.

[15] S. Lemmens and H. Krag, "Two-Line-Elements-Based Maneuver Detection Methods for Satellites in Low Earth Orbit," *Journal of Guidance Control Dynamics*, Vol. 37, May 2014, pp. 860–868, 10.2514/1.61300.

[16] T. Kelecy, D. Hall, K. Hamada, and D. Stocker, "Satellite Maneuver Detection Using Two-line Elements Data," *Advanced Maui Optical and Space Surveillance Technologies Conference*, 2007, p. 19.

[17] A. Morselli, R. Armellin, P. Di Lizia, F. Bernelli-Zazzera, P. D. Lizia, and F. B. Zazzera, "A high order method for orbital conjunctions analysis: Sensitivity to initial uncertainties," *Advances in Space Research*, Vol. 53, No. 3, 2014, pp. 490–508, 10.1016/j.asr.2013.11.038.

[18] C. Levit and W. Marshall, "Improved orbit predictions using two-line elements," *Advances in Space Research*, Vol. 47, Apr. 2011, pp. 1107–1115, 10.1016/j.asr.2010.10.017.

[19] D. Vallado, B. Bastida Virgili, and T. Flohrer, "Improved SSA Through Orbit Determination of Two-Line Element Sets," *6th European Conference on Space Debris, Darmstadt, Germany*.

[20] MATLAB and Optimization Toolbox, *version 8.3.0 (R2014a)*. Natick, Massachusetts: The MathWorks Inc., 2014.

[21] M. J. H. Walker, B. Ireland, and J. Owens, "A set modified equinoctial orbit elements," *Celestial Mechanics*, Vol. 36, No. 4, 1985, pp. 409–419, 10.1007/BF01227493.

[22] J. T. Betts, "Survey of numerical methods for trajectory optimization," *Journal of Guidance, Control and Dynamics*, Vol. 21, No. 2, 1998, pp. 193–207.